



Thermoelectric properties of the $\text{Ru}_2\text{Ni}_2\text{Sb}_{12}$ ternary skutterudite

Jiří Navrátil^{a,*}, František Laufek^{c,b}, Tomáš Plecháček^{c,b,1}, Ľestmír Drašar^{c,b}

^a Institute of Macromolecular Chemistry of the Academy of Sciences of the Czech Republic v.v.i., Heyrovsky sq. 2, 12006 Prague, Czech Republic

^b Czech Geological Survey, Geologická 6, 152 00 Praha 5, Czech Republic

^c Faculty of Chemical Technology, University of Pardubice, 53210 Pardubice, Czech Republic

ARTICLE INFO

Available online 27 March 2012

Keywords:

Ternary skutterudite

$\text{Ru}_2\text{Ni}_2\text{Sb}_{12}$

Thermoelectric properties

Crystal structure

ABSTRACT

The synthesis of the $\text{Ru}_{2-x}\text{Ni}_{2-x}\text{Sb}_{12}$ compounds ($0 \leq x \leq 0.2$), their structural characterization and temperature dependencies of selected transport and thermal properties are reported. At $x=0$, $\text{Ru}_2\text{Ni}_2\text{Sb}_{12}$ displays cubic symmetry, space group $Im\bar{3}$ with lattice parameter $a=9.1767(1)$ Å. From increasing electrical conductivity above 600 K the band gap ($E_g \sim 0.06$ eV) was estimated using an Arrhenius plot. Different signs of the Seebeck coefficient (negative) and the Hall coefficient (positive) have been explained as a consequence of a multicarrier transport. The substitution on a cation site, i.e., formation of the $\text{Ru}_{2-x}\text{Ni}_{2-x}\text{Sb}_{12}$ ternary skutterudites proved to be effective way in suppressing of the thermal conductivity.

© 2012 Elsevier Inc. All rights reserved.

1. Introduction

There is a lot of experimental studies reported in literature in last two decades demonstrating strong potential of materials with skutterudite structure (general formula MX_3 where $M=\text{Co}$, Ir or Rh ; $X=\text{P}$, As or Sb) for advanced thermoelectric applications e.g., [1,2]. Some of the binary skutterudites have good electrical properties, however, they do not demonstrate sufficient thermoelectric performance, because of a relatively high thermal conductivity. The most effective approach in lowering of the high thermal conductivity of skutterudite materials relies on filling empty voids in their crystal structure with heavy atoms, mostly with one e.g., [3] or more rare earth atoms e.g., [4].

Besides traditional approach of lowering of the thermal conductivity by a formation of solid solutions between two or more binary skutterudites, there is also another way to lower lattice part of thermal conductivity of the skutterudite materials, i.e., a formation of ternary skutterudites by an isoelectronic substitution. These ternary skutterudites are materials isoelectronic to the binary skutterudites MX_3 , and can be prepared, e.g., either by an isoelectronic substitution at anionic site X by a pair of elements from 14th to 16th groups (e.g., $\text{CoGe}_{1.5}\text{Se}_{1.5}$ [5], $\text{CoSn}_{1.5}\text{Se}_{1.5}$ [6]), or by an isoelectronic substitution at the cationic site M by a

pair of elements from 8th to 10th groups (e.g., $\text{Fe}_{0.5}\text{Ni}_{0.5}\text{Sb}_3$ [7], $\text{Ru}_{0.5}\text{Pd}_{0.5}\text{Sb}_3$ [8]).

Similar substitution on a cation M-site by a pair of elements from 8th to 10th groups but from different rows of the periodic table led also to synthesis thermodynamically stable ternary skutterudite compounds— $\text{Fe}_2\text{Pd}_2\text{Sb}_{12}$ and $\text{Ru}_2\text{Ni}_2\text{Sb}_{12}$, respectively. The existence of both these compounds is briefly mentioned in Fleurial's list [9] of possible ternary skutterudites. More detailed structure study and basic thermoelectric properties of $\text{Fe}_2\text{Pd}_2\text{Sb}_{12}$ were described by Navrátil et al. in [10].

In this work, we report on preparation and basic structural aspects of $\text{Ru}_{2-x}\text{Ni}_{2+x}\text{Sb}_{12}$ ($x=0, 0.1, 0.2$) compounds. The effect of cation substitution on transport and thermoelectric properties is also reported.

2. Experimental

2.1. Synthesis and thermal analysis

The $\text{Ru}_{2-x}\text{Ni}_{2+x}\text{Sb}_{12}$ ($x=0, 0.1, 0.2$) ternary compounds were synthesized from elemental powders by high-temperature solid-state reactions. Ni powder was first heated at 600 °C for 2 h in H_2 atmosphere to reduce possible oxides. The stoichiometric amounts of Ru (99.9%), Ni (99.9%) and Sb (99.999%) were sealed into evacuated silica glass tubes and heated at 1050 °C for 48 h in a furnace. The material was then ground under acetone using agate mortar and pestle and heated at 500 °C for 168 h. The resultant material was once again ground under acetone and heated again at 500 °C for 240 h. After the heat treatment, the furnace was turned off and allowed to cool slowly to room

* Corresponding author at University of Pardubice, Institute of Macromolecular Chemistry of the Academy of Sciences, Joint Laboratory of Solid State Chemistry, 53210 Pardubice, Czech Republic. Fax: +420 466036011.

E-mail address: Jiri.Navratil@upce.cz (J. Navrátil).

¹ Present address: Joint Laboratory of Solid State Chemistry of Institute of Macromolecular Chemistry of the Academy of Sciences of the Czech Republic v.v.i. and the University of Pardubice, 53210 Pardubice, Czech Republic

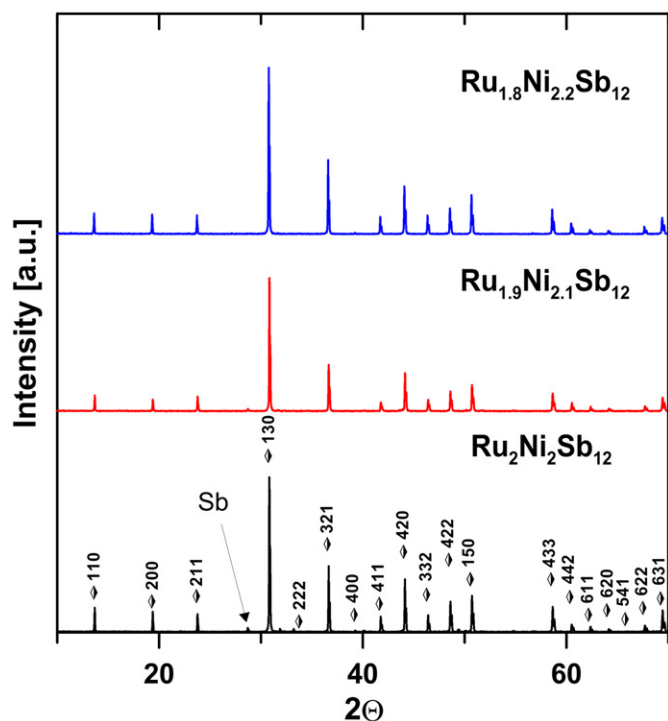


Fig. 1. Powder X-ray diffraction patterns of the prepared $\text{Ru}_{2-x}\text{Ni}_{2+x}\text{Sb}_{12}$ compounds (CuK_α radiation). (For interpretation of the references to color in this figure legend, the reader is referred to the web version of this article.)

temperature. Finally, obtained powder samples were, after verification of the completion of the solid-state reaction with powder X-ray diffraction, hot-pressed at 500 °C (HP-samples) and 80 MPa for 1 h. The powder X-ray diffraction patterns of the prepared samples are shown in Fig. 1.

The differential thermal analysis (DTA) was carried out using the instrument R.M.I.–DTA 003 (Electronic Measuring Instruments) at a non-isothermal regime in the temperature range 300–1070 K. Small quartz ampoule with powdered sample (about 40 mg of weight) was evacuated down to 10^{-3} Pa and heated with rate of 10 K min^{-1} . The calibration was made with the help of In, Al, Zn, Pb and Sn in order to eliminate the differences between the temperature of the thermocouples in the furnace and in the vicinity of the sample. Pure Al_2O_3 was used as a standard. The heating DTA curves of the studied samples obtained under above given conditions are presented in Fig. 2.

2.2. Crystal structure refinement

The powder X-ray diffraction patterns of $\text{Ru}_{2-x}\text{Ni}_{2+x}\text{Sb}_{12}$ ($x=0, 0.1, 0.2$) ternary compounds were collected in the Bragg–Brentano geometry on a Bruker D8 Advance diffractometer. CuK_α radiation was used. The details of data collection and basic crystallographic facts for $\text{Ru}_2\text{Ni}_2\text{Sb}_{12}$ are given in Table 1.

The crystal structures of $\text{Ru}_{2-x}\text{Ni}_{2+x}\text{Sb}_{12}$ ($x=0, 0.1, 0.2$) phases were refined by the Rietveld method for X-ray powder diffraction data using the FullProf program [11]. All synthesized phases were found to be isostructural with the cubic skutterudite structure CoSb_3 ($Im\bar{3}$ symmetry). As follows from Fig. 1, a small amount of unreacted antimony (ca 3 wt%) was detected in $\text{Ru}_2\text{Ni}_2\text{Sb}_{12}$ and $\text{Ru}_{1.9}\text{Ni}_{2.1}\text{Sb}_{12}$ samples. The refined parameters contain those describing peak shape and width, peak asymmetry (2 parameters), unit cell parameter and fractional coordinates. The pseudo-Voigt function was employed to model the line shape of diffraction profiles. The background was determined by linear interpolation between

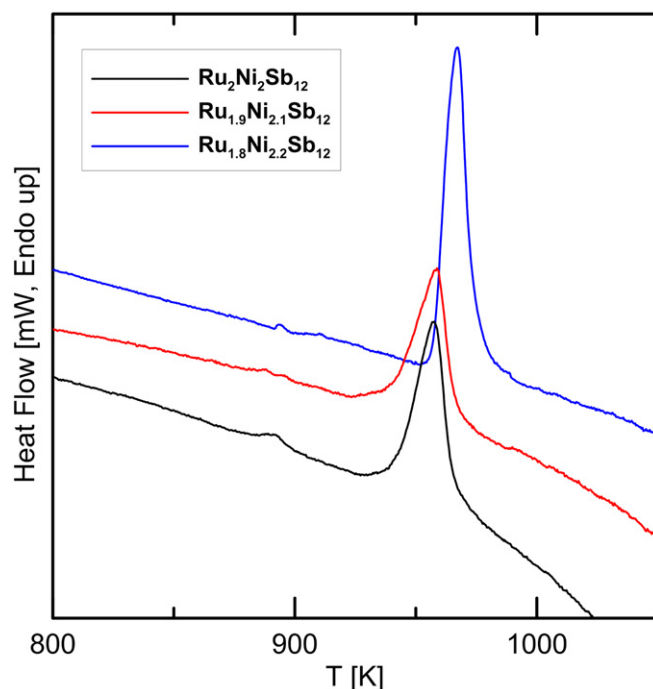


Fig. 2. The heating DTA curves of the $\text{Ru}_{2-x}\text{Ni}_{2+x}\text{Sb}_{12}$ compounds. (For interpretation of the references to color in this figure legend, the reader is referred to the web version of this article.)

Table 1

Data collection and Rietveld analysis for $\text{Ru}_2\text{Ni}_2\text{Sb}_{12}$. R agreement factors defined according to [16].

Data collection	
Radiation type, source	X-ray, CuK_α
Generator settings	40 kV, 40 mA
Data collection temperature	room temperature
Range in 2θ (°)	10–110
Step size (°)	0.02
Crystal data	
Space group	$Im\bar{3}$ (No. 204)
Unit cell content	$\text{Ru}_{0.5}\text{Ni}_{0.5}\text{Sb}_3$, $Z=8$
Unit cell parameters (Å)	$a=9.1767(1)$
Rietveld analysis	
No. of reflections	102
No. of structural parameters	2
No. of profile parameters	6
R_{Bragg}	0.063
R_p	0.084
R_{wp}	0.010
Weighting scheme	$1/y_o$

consecutive breakpoints in the diffraction pattern. Finally, 14 parameters were allowed to vary. The Ru and Ni atoms randomly occupy the 8c position of the $Im\bar{3}$ space group; no indications of structural ordering were observed. The final Rietveld plot is depicted in Fig. 3, Tables 2 and 3 show refined structural parameters for $\text{Ru}_2\text{Ni}_2\text{Sb}_{12}$ phase and calculated lattice parameters for $\text{Ru}_{2-x}\text{Ni}_{2+x}\text{Sb}_{12}$ ($x=0, 0.1, 0.2$) compounds.

2.3. Thermoelectric properties measurements

Electrical conductivity was measured with four-probe method using Lock-in Amplifier (EG&G model 5209) on the rectangular parallelepiped of dimensions about $15 \times 3.5 \times 2 \text{ mm}^3$. The measurements were performed on two probes, one in the temperature region from about 100–350 K and the other from 300 to 800 K. On the same samples Hall effect measurements were carried out over

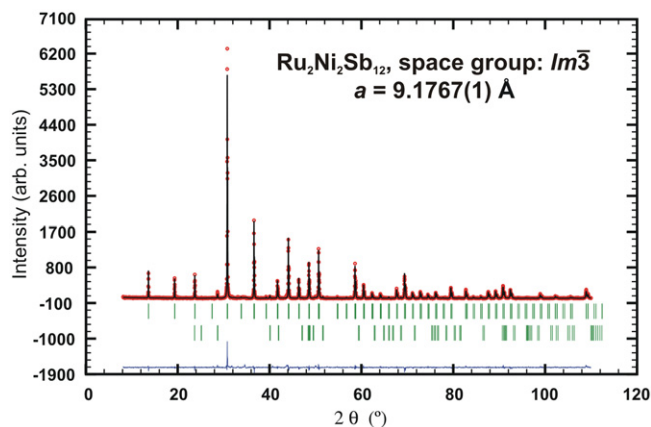


Fig. 3. Observed (circles), calculated (solid line) and difference Rietveld profiles for $\text{Ru}_2\text{Ni}_2\text{Sb}_{12}$. The upper reflection bars correspond to $\text{Ru}_2\text{Ni}_2\text{Sb}_{12}$ and the lower bars to a 3 mass percent Sb impurity. (For interpretation of the references to color in this figure legend, the reader is referred to the web version of this article.)

Table 2

Refined atomic coordinates for the $\text{Ru}_2\text{Ni}_2\text{Sb}_{12}$.

Atom	Site	x	y	z	Occ.	B_{iso} (Å^2)
Ru	8c	1/4	1/4	1/4	0.5	0.94(9)
Ni	8c	1/4	1/4	1/4	0.5	0.94(9)
Sb	24g	0	0.3379(2)	0.1556(2)	1	0.67(3)

Table 3

Lattice parameters and unit-cell volume for $\text{Ru}_{2-x}\text{Ni}_{2+x}\text{Sb}_{12}$ ($x=0, 0.1, 0.2$) studied samples.

Weighted composition	a (Å)	V (Å^3)
$\text{Ru}_2\text{Ni}_2\text{Sb}_{12}$	9.1767(1)	772.79(1)
$\text{Ru}_{1.9}\text{Ni}_{2.1}\text{Sb}_{12}$	9.1762(2)	772.66(3)
$\text{Ru}_{1.8}\text{Ni}_{2.2}\text{Sb}_{12}$	9.1757(2)	772.53(3)

the temperature range 100–400 K, using an alternating current of the frequency of 1020 Hz and stationary magnetic field of an induction $B=0.7$ T. The ohmic current contacts were made by means of sputtered Au layer and Ag-conductive paste. The mechanical contacts for measuring the Hall voltage were used.

The Seebeck coefficient was determined by means of static dc method on rectangular shaped samples. The temperature gradient between two points was measured by two shielded K-type thermocouples that were pressed against the sample surface. A potential difference dU corresponding to the gradient dT was measured across the same legs of both attached thermocouples. The absolute Seebeck coefficient was determined from the slope of dU/dT dependence using 20 values of dT not exceeding 3 K. The thermal diffusivity was measured on round hot-pressed sample with help of LFA 457 (Netzsch). The thermal conductivity was then calculated using Pyroceram 9606as a heat capacity standard.

3. Results and discussion

3.1. Crystal structure of $\text{Ru}_{2-x}\text{Ni}_{2+x}\text{Sb}_{12}$ samples

The $\text{Ru}_{2-x}\text{Ni}_{2+x}\text{Sb}_{12}$ ($x=0, 0.1, 0.2$) phases show the skutterudite-type structure. Their crystal structures can be described as an infinite array of [(Ni/Ru)Sb₆] octahedra sharing corners with six neighboring octahedra (Fig. 4(a)). The tilt system $a^+a^+a^+$ of

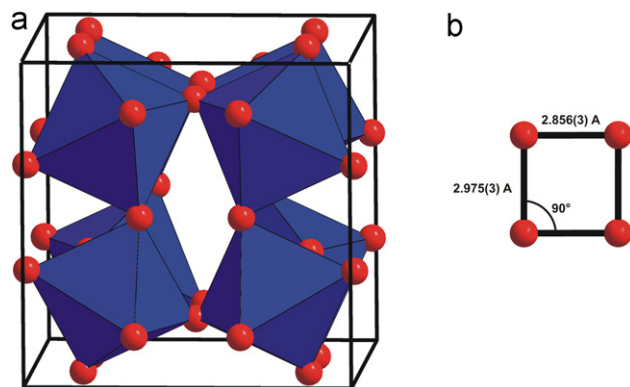


Fig. 4. (a) Polyhedral representation of $\text{Ru}_2\text{Ni}_2\text{Sb}_{12}$ crystal structure. The [Ru/NiSb₆] corner-sharing octahedra are emphasized. (b) The four-membered ring in $\text{Ru}_2\text{Ni}_2\text{Sb}_{12}$. (For interpretation of the references to color in this figure legend, the reader is referred to the web version of this article.)

the original skutterudite structure is preserved. The skutterudite structure can be viewed as a derivative of the perovskite structure, characterized by elimination of the A atoms and by tilting of the BX_6 octahedra [12,13]. The tilt angle (φ) can be calculated from the unit-cell parameter a and the M–X distance according to a relationship: [14]

$$\cos(\varphi) = \frac{3a}{8d} - 0.5 \quad (1)$$

The calculated value of octahedral tilt for $\text{Ru}_2\text{Ni}_2\text{Sb}_{12}$ phase is 33.6° , which can be compared to the value of 33.7° found $\text{Pd}_2\text{Ni}_2\text{Sb}_{12}$ [10]. This value of the octahedral tilt falls between values calculated from binary Sb-bearing skutterudites CoSb_3 (32.4°) [7] and IrSb_3 (34.3°) [7]. Considering the covalent radii of Ni, Co, Pd, Rh and Ir, these numbers of tilt angles support the general trend observed in skutterudites: for a given anion, the tilt angle (φ) increases with the increasing size of the cation [12].

As is typical for the skutterudite structure, the Sb atoms in $\text{Ru}_2\text{Ni}_2\text{Sb}_{12}$ form the four-membered rings [Sb₄] of rectangular shape (Fig. 4(b)). The short (2.856 Å) and long (2.975 Å) Sb–Sb distances alternate within these [Sb₄] rings (Fig. 4(b)). The ratio between these two Sb–Sb distances is 1.04, which falls between values observed for unfilled binary skutterudites (1.03–1.05) [7].

3.2. Thermoelectric and thermal properties

DTA measurement, which was carried out on the studied samples (see Fig. 2), revealed a strong endo-thermic peak at about 950–960 K, which is undoubtedly connected with decomposition of the compounds. This is the reason why all experiments were carried out up to maximal temperature of 800 K. Sb, NiSb_2 and very likely RbSb_2 were identified as breakdown products after DTA-treatment. One smaller endo-thermic peak visible in DTA curve at about 900 K corresponds to the melting of the residual unreacted Sb (see Fig. 1).

The temperature dependencies of the electrical conductivity σ of $\text{Ru}_{2-x}\text{Ni}_{2+x}\text{Sb}_{12}$ ($x=0, 0.1, 0.2$) samples are presented in Fig. 5. From this figure it is evident that electrical conductivities of all studied samples initially decrease, reach a minimum, and then increase with the increasing temperature. The increase of σ at $T > 600$ K is related to the transition of electrons across a band gap. This is a typical feature for heavily doped narrow band-gap semiconductors. Fig. 6 shows σ as a function of reciprocal temperature. An exponential fit $\sigma = \sigma_0 \cdot \exp(E_g/2kT)$ of these dependencies in the area of increasing conduction provides value of activation energy E_g connected with the above mentioned

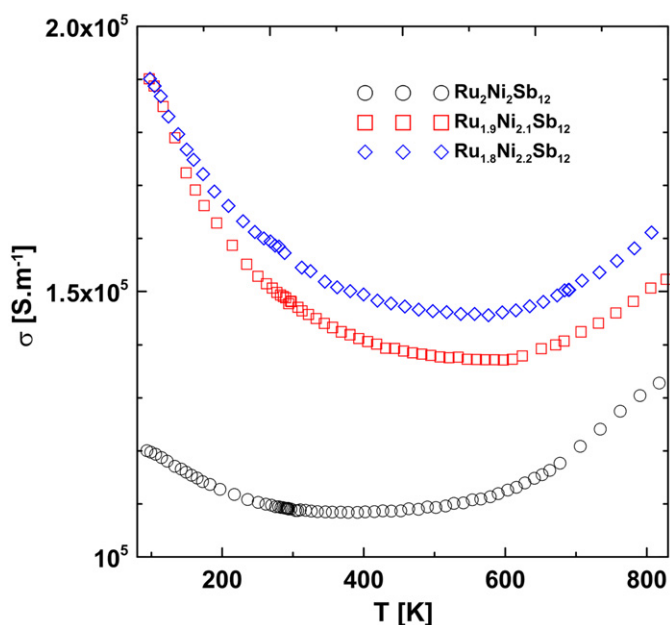


Fig. 5. Temperature dependencies of electrical conductivity σ of $\text{Ru}_{2-x}\text{Ni}_{2+x}\text{Sb}_{12}$ samples. (For interpretation of the references to color in this figure legend, the reader is referred to the web version of this article.)

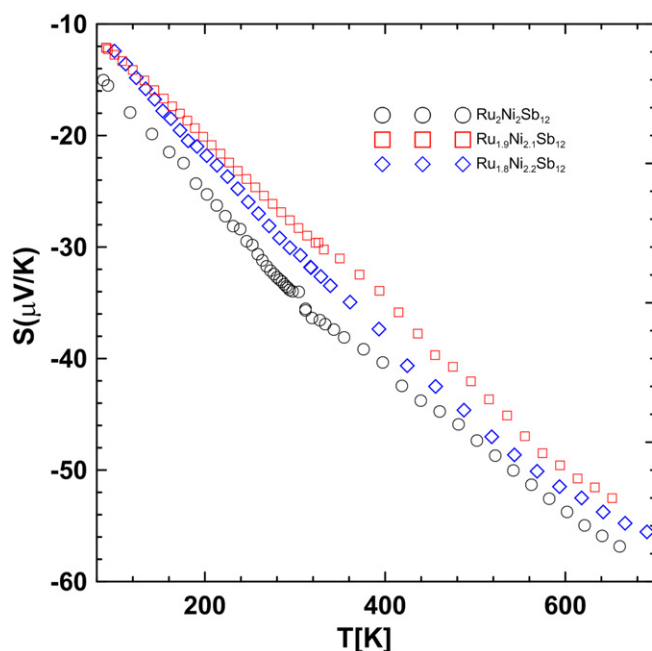


Fig. 7. Temperature dependencies of the Seebeck coefficient S of $\text{Ru}_{2-x}\text{Ni}_{2+x}\text{Sb}_{12}$ samples. (For interpretation of the references to color in this figure legend, the reader is referred to the web version of this article.)

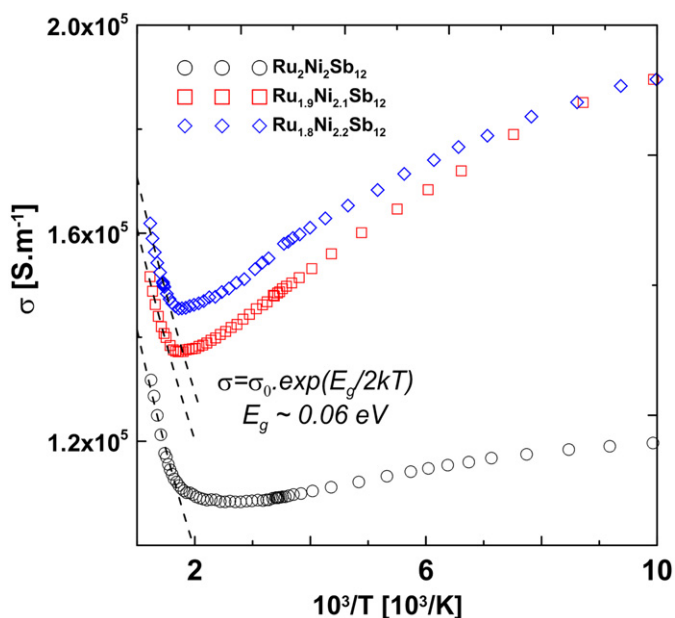


Fig. 6. Electrical conductivity σ versus inverse temperature for $\text{Ru}_{2-x}\text{Ni}_{2+x}\text{Sb}_{12}$ samples. (For interpretation of the references to color in this figure legend, the reader is referred to the web version of this article.)

transition. It is approximately the same for all samples, i.e., about 0.06 eV. Using the same procedure we obtained for analogical skutterudite compound $\text{Fe}_2\text{Pd}_2\text{Sb}_{12}$ the value about 0.22 eV [10]. The other related compound, $\text{Fe}_2\text{Ni}_2\text{Sb}_{12}$, has value of E_g about 0.16 eV [9].

Another important finding comes from the comparison of temperature dependencies of the Seebeck coefficient (Fig. 7) and the Hall coefficient (Fig. 8) of the prepared samples. The negative values of Seebeck coefficient for all samples in the whole observed temperature region reflect prevailing n-type form of electron transport. As expected, samples with higher electrical

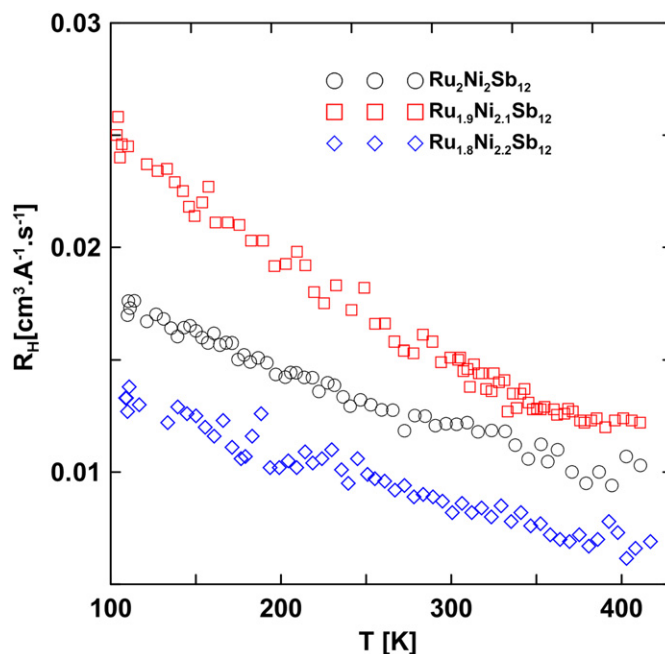


Fig. 8. Temperature dependencies of the Hall coefficient R_H of $\text{Ru}_{2-x}\text{Ni}_{2+x}\text{Sb}_{12}$ samples. (For interpretation of the references to color in this figure legend, the reader is referred to the web version of this article.)

conductivity have lower Seebeck coefficients and vice versa. Contrary to the n-type character of their Seebeck coefficient all samples exhibit positive values of their Hall coefficient. This is not surprising since a similar behavior was observed also for $\text{Fe}_2\text{Ni}_2\text{Sb}_{12}$ compound [9] and very complex behavior of the both properties was presented for $\text{Fe}_2\text{Pd}_2\text{Sb}_{12}$ [10]. Different signs of the Seebeck and Hall coefficients are usually the sign of a multi-carrier nature of transport consisting of at least one type of electrons and one type of holes, which participate in the conduction process and hence mixed conduction prevails in carrier transport.

In such a two-carrier system, the Seebeck coefficient is expressed as

$$S = \frac{S_e n \mu_e + S_h p \mu_h}{n \mu_e + p \mu_h} \quad (2)$$

where e is the charge of the carrier, p and n are the partial carrier concentrations, μ_e and μ_h are the electron and hole mobility and S_e and S_h are the partial electron and hole Seebeck coefficients. Therefore, the Seebeck coefficient is determined by both concentration and mobility of carriers. In the case of the Hall coefficient, it is the sum of quadratic terms in the carrier mobility, as given by following expression:

$$R_H = \frac{-n \mu_e^2 + p \mu_h^2}{e(n \mu_e + p \mu_h)^2} \quad (3)$$

Thus, the Hall coefficient can have an opposite sign with respect to the Seebeck coefficient. In the case of skutterudites the hole mobility is much higher than that of electrons e.g., [15] and thus R_H value can be positive, even though the concentration of electrons exceeds the concentration of holes. This fact follows from Eq. (2) and from the negative sign of measured Seebeck coefficient. Since we deal with more than one group of carriers, we cannot deduce the concentration of carriers from the Hall coefficient directly. Hall mobility, or more precisely in this case product of $R_H \cdot \sigma$, of the studied samples reach values of a few tens of $\text{cm}^2 \text{V}^{-1} \text{s}^{-1}$ (see Fig. 9). Their temperature dependencies resemble similar dependence published for $\text{Ru}_2\text{Pd}_2\text{Sb}_{12}$ compound [8]. Due to the above mentioned coexistence of at least two types of carriers one cannot make any conclusions on dominant scattering mechanism from the dependencies just due to the above mentioned multicarrier nature of the transport phenomena.

Thermal conductivity of $\text{Ru}_2\text{Ni}_2\text{Sb}_{12}$ (see Fig. 10) is in the measured temperature region (300–650 K) almost constant with value about $3.5 \text{ W m}^{-1} \text{ K}^{-1}$, i.e., about four times lower than reported value for $\text{Ru}_{0.5}\text{Pd}_{0.5}\text{Sb}_3$ compound [8] and approximately the same value as for related skutterudite compound $\text{Fe}_2\text{Pd}_2\text{Sb}_{12}$ [10]. Assuming validity of the Wiedemann–Franz law (with the

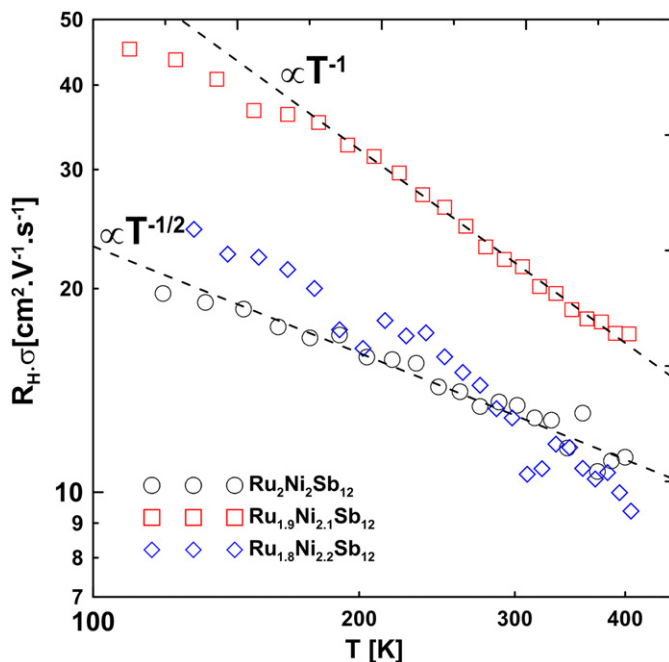


Fig. 9. Product $R_H \cdot \sigma$ vs. temperature for $\text{Ru}_{2-x}\text{Ni}_{2+x}\text{Sb}_{12}$ samples. (For interpretation of the references to color in this figure legend, the reader is referred to the web version of this article.)

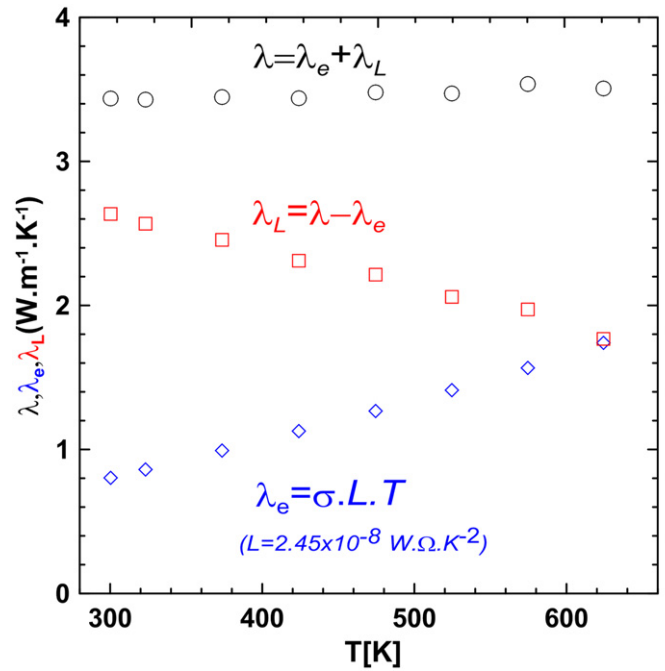


Fig. 10. Thermal conductivity λ and its lattice λ_L and electronic λ_e components versus temperature for $\text{Ru}_2\text{Ni}_2\text{Sb}_{12}$ sample. (For interpretation of the references to color in this figure legend, the reader is referred to the web version of this article.)

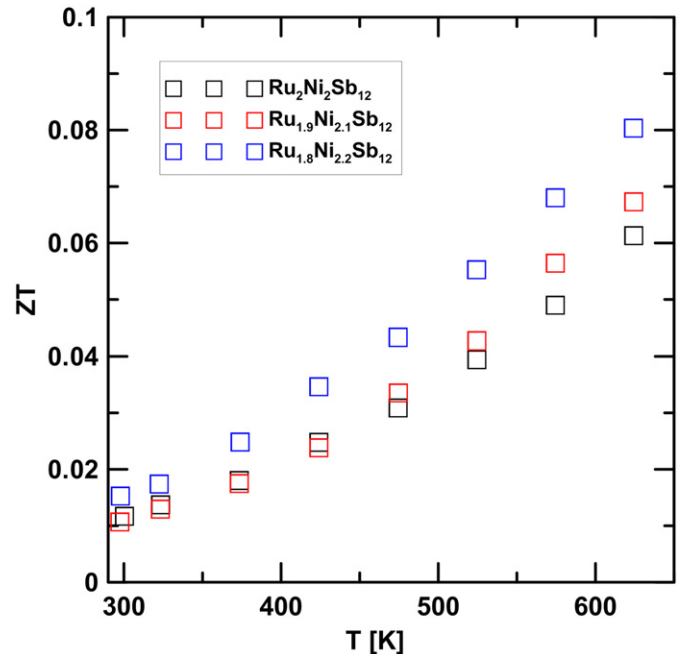


Fig. 11. Temperature dependencies of calculated ZT values of $\text{Ru}_{2-x}\text{Ni}_{2+x}\text{Sb}_{12}$ samples. (For interpretation of the references to color in this figure legend, the reader is referred to the web version of this article.)

Lorenz number $L_0 = 2.45 \times 10^{-8} \text{ W K}^{-1}$) we calculated electronic part of thermal conductivity and after subtraction of the values from total thermal conductivity we obtained its lattice component. Its value decreases with increasing temperature from about $2.5 \text{ W m}^{-1} \text{ K}^{-1}$ (300 K) down to $\sim 1.5 \text{ W m}^{-1} \text{ K}^{-1}$ (650 K). Values of the total thermal conductivity of the other two studied compounds slightly decrease with increasing Ni content, i.e., $3.2 \text{ W m}^{-1} \text{ K}^{-1}$ at 300 K for $\text{Ru}_{1.9}\text{Ni}_{2.1}\text{Sb}_{12}$ and $2.9 \text{ W m}^{-1} \text{ K}^{-1}$ at 300 K for $\text{Ru}_{1.8}\text{Ni}_{2.2}\text{Sb}_{12}$.

Thermoelectric properties of the samples are significantly degraded due to the participation of comparable quantities of electrons and holes on electronic transport. The fact seems to be a reason of low ZT values (Fig. 11) calculated for the studied samples. They achieve maximal value $ZT \sim 0.08$ at 630 K for $\text{Ru}_{1.8}\text{Ni}_{2.2}\text{Sb}_{12}$ sample. The suppression of the concentration of either electrons or holes could lead to an improvement of the thermoelectric properties.

4. Conclusion

Cation-substituted ternary skutterudite $\text{Ru}_{2-x}\text{Ni}_{2+x}\text{Sb}_{12}$ ($x=0, 0.1, 0.2$) samples were prepared and their skutterudite-type structure with space group $Im\bar{3}$ was confirmed. No indications of structural ordering were found. Anomalous behavior, i.e., different signs of Seebeck and Hall coefficient was attributed to the multi-carrier nature of the electronic transport in the studied compounds. The compounds exhibit a low value of lattice part of thermal conductivity, i.e., about $1.5 \text{ W m}^{-1} \text{ K}^{-1}$ at 650 K. Suppression of the intrinsic regime by proper doping might lead to significant improvement of thermoelectric properties of the compound.

Acknowledgments

Financial support from the Grant Agency of the Czech Republic (GA CR), project no. P108/10/1315, from the Ministry of Education of the Czech Republic project MSM0021627501 and from

the Czech Geological Survey (project no. 332300) is greatly appreciated.

References

- [1] C. Uher, Chemistry, in: M.G. Kanatzidis, S.D. Mahanti, T.P. Hogan (Eds.), *Physics and Materials Science of Thermoelectric Materials: Beyond Bismuth Telluride*, Plenum, New York, 2003, pp. 121–147.
- [2] Jiong Xun Shi, James R. Yang, Miaofang Salvador, Jung Y. Chi, Hsin Cho, Shengqiang Wang, Jihui Bai, Wenqing Yang, Zhang, Lidong Chen, *J. Am. Chem. Soc.* 133 (20) (2011) 7837–7846.
- [3] B.C. Sales, D. Mandrus, R.K. Williams, *Science* 272 (5266) (1996) 1325–1328.
- [4] C. Uher, Chang-Peng Li, S. Ballikaya, *J. Electron.Mater.* 39 (9) (2010) 2122–2126.
- [5] G.S. Nolas, J. Yang, R.W. Ertenberg, *Phys. Rev. B* 68 (19) . 193206–4.
- [6] F. Laufek, J. Navratil, J. Plašil, T. Plecháček, Č. Drašar, *J. Alloys Compd.* 479 (2009) 102–106.
- [7] A. Kjekshus, T. Rakke, *Acta Chem. Scand. A* 28 (1974) 99–103.
- [8] T. Caillat, J. Kulleck, A. Borshchevsky, J.P. Fleurial, *Appl. Phys.* 79 (1996) 8419–8426.
- [9] J.P. Fleurial, T. Caillat, and A. Borshchevsky, *Proceedings of the 14th International Conference on Thermoelectrics*, St. Petersburg, Russia, June 1995, pp. 231–235.
- [10] J. Navrátil, F. Laufek, T. Plecháček, J. Plášil, *J. Alloys Compd.* 493 (1–2) (2010) 50–54.
- [11] J. Rodríguez-Carvajal, FullProf.2k Rietveld Profile Matching & Integrated Intensities Refinement of X-ray and/or Neutron Data (Powder and/or Single-Crystal), Laboratoire Léon Brillouin, Centre d'Etudes de Saclay, Gif-sur-Yvette Cedex, France, 2006.
- [12] R.H. Mitchell, *Perovskites: Modern and Ancient*, Almaz Press, Thunder Bay, Ontario, 2002.
- [13] P. Vaquero, G.G. Sobany, M. Stindl, *J. Solid State Chem.* 181 (2008) 768–776.
- [14] M. O'Keefe, B.G. Hyde, *Acta Crystallogr. B* 33 (1977) 3802–3813.
- [15] T. Caillat, A. Borshchevsky, J.-P. Fleurial, *J. Appl. Phys.* 80 (1996) 4442–4449.
- [16] L.B. McCusker, R.B. von Dreele, D.E. Cox, D. Louër, P. Scardi, *J. Appl. Cryst.* 32 (1999) 36.